ChemPubSoc Europe

DOI: 10.1002/open.201402097

Open Access ChemistryOPEN Full Papers

Site-Specific Radioiodination of HER2-Targeting Affibody Molecules using 4-Iodophenethylmaleimide Decreases Renal Uptake of Radioactivity

Joanna Strand,[a] Patrik Nordeman,[b] Hadis Honarvar,[a] Mohamed Altai,[a] Anna Orlova,[b] Mats Larhed,[b] and Vladimir Tolmachev*[a]

Affibody molecules are small scaffold-based affinity proteins with promising properties as probes for radionuclide-based molecular imaging. However, a high reabsorption of radiolabeled Affibody molecules in kidneys is an issue. We have shown that the use of ^{125}I-3-iodo-((4-hydroxyphenyl)ethyl)maleimide (IHPEM) for site-specific labeling of cysteine-containing Affibody molecules provides high tumor uptake but low radioactivity retention in kidneys. We hypothesized that the use of 4-iodophenethylmaleimide (IPEM) would further reduce renal retention of radioactivity because of higher lipophilicity of radiometabolites. An anti-human epidermal growth factor receptor type 2 (HER2) Affibody molecule ($Z_{HER2:2395}$) was labeled using ^{125}I-IPEM with an overall yield of 45 ± 3%. ^{125}I-IPEM-$Z_{HER2:2395}$ bound specifically to HER2-expressing human ovarian carcinoma cells (SKOV-3 cell line). In NMRI mice, the renal uptake of ^{125}I-IPEM-$Z_{HER2:2395}$ (24 ± 2 and 5.7 ± 0.3% IA g^{-1} at 1 and 4 h after injection, respectively) was significantly lower than uptake of ^{125}I-IHPEM-$Z_{HER2:2395}$ (50 ± 8 and 12 ± 2% IA g^{-1} at 1 and 4 h after injection, respectively). In conclusion, the use of a more lipophilic linker for the radioiodination of Affibody molecules reduces renal radioactivity.

Introduction

Malignant transformation is often associated with an aberrant expression of certain types of cell-surface proteins, for example, receptors, cell adhesion molecules, or proteins active in embryonic development.[1] Molecular recognition of these proteins can be used for specific treatment of malignant cells, for example, targeted therapy. Monoclonal antibodies (Mabs) are the most used kind of targeting agents, which may act by preventing mitogenic signaling[2] or by eliciting antibody-dependent or complement-dependent cytotoxicity.[3] Antitumor action of Mabs might be further enhanced by conjugation of cytotoxic drugs or radionuclides.[4] However, there is an appreciable inter- and intrapatient heterogeneity in expression of molecular targets. Apparently, tumors that do not express particular targets would not respond to a particular targeting therapy. Therefore, the targeted treatment should be personalized, that is, adjusted to the tumor molecular abnormality profile of each particular cancer case.[5] In vivo visualization of cell-surface target proteins using radionuclide molecular imaging can personalize anticancer treatment by the selection of patients who would most likely benefit from a particular targeted therapy.[6]

A possible approach to the development of imaging agents is the radiolabeling of therapeutic Mabs using nuclides emitting gamma quanta that can be detected outside the patient's body.[7] The use of Mabs as imaging agents has, however, certain downsides. Antibodies are relatively bulky proteins (150 kDa); this limits their rates of extravasation, tumor penetration, and blood clearance of unbound tracers.[7,8] Therefore, imaging is possible only several days after injection. In addition, antibodies have a tendency to accumulate in tumors nonspecifically due to an "enhanced permeability and retention" (EPR) effect, which might cause false positive diagnoses.[7] Small engineered scaffold affinity proteins, for example, Affibody molecules, are strong alternatives to antibodies in the development of imaging agents.[9] Affibody molecules are small (7 kDa) three-helical cysteine-free scaffold proteins derived from the immunoglobulin-binding B domain of staphylococcal receptor protein A.[10] Randomization of surface amino acids on helices 1 and 2 of Affibody molecules creates large combinatorial libraries enabling the selection of high-affinity binders to different proteins, including cancer-associated ones.[10] The small size and high affinity (in low nanomolar and subnanomolar range) makes them good candidates for development of imaging probes.[11] Affibody-based agents have been generated for the imaging of several cancer-associated molecular targets, for example human epidermal growth factor receptor type 2 (HER2),[12] insulin-like growth factor-1 receptor

[a] J. Strand, H. Honarvar, Dr. M. Altai, Prof. Dr. V. Tolmachev
Biomedical Radiation Sciences, Faculty of Medicine
Uppsala University, 751 85 Uppsala (Sweden)
E-mail: vladimir.tolmachev@bms.uu.se

[b] Dr. P. Nordeman, Dr. A. Orlova, Prof. Dr. M. Larhed
Preclinical PET Platform, Department of Medicinal Chemistry
Faculty of Pharmacy, Uppsala University, 751 23 Uppsala (Sweden)

ORCID(s) from the author(s) for this article is/are available on the WWW under http://dx.doi.org/10.1002/open.201402097.

(IGF-1R),[13] platelet derived growth factor beta (PDGFβ),[14] epidermal growth factor receptor (EGFR),[15] and carbonic anhydrase IX (CAIX).[16] Preclinical studies have demonstrated that Affibody molecules provide a much higher contrast than radiolabeled Mabs and enable imaging only a few hours after injection.[17] Clinical studies have demonstrated the capacity of Affibody molecules to image HER2 expression in breast cancer metastases.[18,19]

The major excretion route of Affibody molecules is renal due to their small size. After glomerular filtration, Affibody molecules undergo nearly quantitative reabsorption in the renal tubuli cells followed by internalization and lysosomal degradation. The use of residualizing radiometal labels results in a long retention of radioactivity in kidneys. This phenomenon was observed for Affibody molecules specific to different targets, for example, HER2, IGF-1R, EGFR, and PDGFRβ, and labeled with different radiometals using different chelators.[13,14,15,20,21] The high renal retention is a major dosimetry problem in the case of radionuclide therapy and might complicate imaging of metastases in the lumbar region. On the other hand, radiocatabolites are cleared rapidly from kidneys when Affibody molecules are labeled using nonresidualizing halogens, such as ^{18}F,[22,23,24] ^{76}Br,[25] or different iodine radioisotopes.[17,26,27] Importantly, internalization of receptor-bound Affibody molecules by cancer cells is slow,[13,14,15,28] which makes residualizing properties of a label not critical for successful targeting. Thus, the use and further development of nonresidualizing labels is a promising way to reduce renal retention of radioactivity of radiolabeled Affibody molecules.

Among radiohalogens, iodine radioisotopes offer a variety of properties as labels for targeting proteins and peptides; for example, ^{123}I ($t_{1/2}$ = 13.3 h) is suitable for imaging using single-photon emission computed tomography (SPECT), ^{124}I ($t_{1/2}$ = 4.18 d) for positron emission tomography (PET), and ^{131}I ($t_{1/2}$ = 8 d) for therapy. The long-lived ^{125}I ($t_{1/2}$ = 59.4 d) is a convenient surrogate nuclide, which is commonly used in the development of radioiodination techniques. Direct radioiodination of Affibody molecules destroys binding, presumably due to the presence of tyrosine in the binding site.[28] To overcome this problem, Affibody molecules were indirectly labeled using *N*-succinimidyl *para*-iodobenzoate (SPIB) as a precursor.[12] The resulting ^{125}I -*para*-iodobenzoate (^{125}I-PIB)-$Z_{HER2:342}$ has demonstrated high-contrast imaging of HER2-expressing xenografts in mice and low renal retention of radioactivity. A disadvantage of that method is that it is not site-specific. There are seven amino groups in $Z_{HER2:342}$ (*N*-terminus and six lysines), which result in a mixture of proteins with a different number of labeled prosthetic groups per protein at different positions. A meta-analysis of biodistribution studies suggested that the biodistribution profile of (^{125}I-PIB)-$Z_{HER2:342}$ was not quite reproducible, possibly because of some deviation in labeling conditions resulting in different compositions of such a mixture.[26]

The introduction of a unique thiol group by engineering a cysteine into the Affibody molecule allows a site-specific coupling of a linker molecule by thiol-directed chemistry. Both indirect radiohalogenation of cysteine-containing Affibody molecules using 3-bromo-(4-hydroxyphenethyl)maleimide (BrHPEM) or 3-iodo-(4-hydroxyphenethyl)maleimide (IHPEM) (**1**, Figure 1) as an intermediate precursor resulted in a homogenous radiolabeled product with preserved binding specificity.[25,27] Surprisingly, the use of BrHPEM and IHPEM resulted in four to sevenfold decrease of renal retention of radioactivity at 4 h after injection, in comparison with the use of *para*-halobenzoate-based labels. This demonstrated that positioning of the linker molecule influences the biodistribution profile. However, the exact mechanism of the decrease is not clear. We speculate that exoproteases are predominantly featured in the renal proteolysis of Affibody molecules, and a terminal placement results in a more rapid formation of "leaky" lipophilic radiometabolites. As lipophilicity of radiometabolites is an important factor in their decreased intracellular retention,[29] the use of a more lipophilic pendant group for C-terminal radioiodination of cysteine-containing Affibody molecules should further reduce renal retention of radioactivity. *N*-(4-[^{125}I]iodophenethyl)maleimide (^{125}I-IPEM) (**2**), which has been earlier developed for site-specific labeling of antigen-binding fragments (Fab fragments),[30] would be a suitable linker, as it both permits site-specific labeling of cysteine-containing Affibody molecules and is more lipophilic than IHPEM.

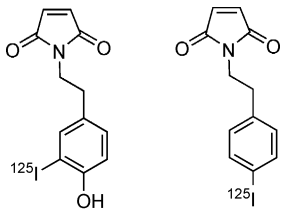

Figure 1. Structures of ^{125}I-3-iodo-((4-hydroxyphenyl)ethyl)maleimide (^{125}I-IHPEM) (**1**) and ^{125}I-4-iodophenethylmaleimide (^{125}I-IPEM) (**2**).

The goal of this study was to test hypothesis that the use of ^{125}I-IPEM for indirect radioiodination of Affibody molecules provides a conjugate that is capable of specific binding to its molecular target cells and provides lower renal retention of radioactivity than its ^{125}I-IHPEM-labeled counterpart. The anti-HER2 Affibody molecule $Z_{HER2:2395}$ with a C-terminal cysteine was used as a model in this study. Labeling of $Z_{HER2:2395}$ using ^{125}I-IPEM was established, and properties of ^{125}I-IPEM-$Z_{HER2:2395}$ and ^{125}I-IHPEM-$Z_{HER2:2395}$ were directly compared in vitro and in vivo.

Results and Discussion

Synthesis of *N*-[4-(tri-*n*-butylstannylphenethylamine)phenethyl]maleimide (7)

Synthesis of a precursor for iododestannylation, *N*-[4-(tri-*n*-butylstannyl)phenethyl]-maleimide (**7**), was performed according to Scheme 1. 4-Bromophenethylamine (**3**) was protected with phthalimde using phthalic anhydride and provided **4** in 81%. A palladium-catalyzed metal–halogen exchange using bis(tributyltin) yielded **5** in 83%. Deprotection of the phthalamide group using methylamine (94% yield) and a subsequent reaction with malemide provided **7** in 30%. Synthesis of nonradioactive iodophenethylmaleimide (**8**) for the use as a chroma-

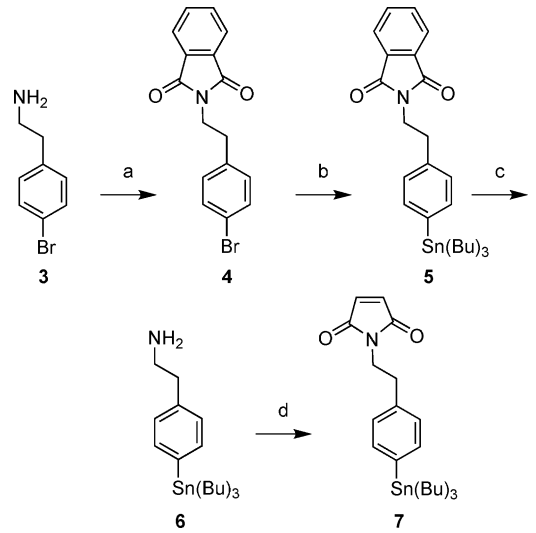

Scheme 1. *Reagents and conditions*: a) phthalic anhydride, Et_2O, rt, 2 h, then glacial HOAc, 65 °C, 81 %; b) **4a**, 2 % $Pd(PPh_3)_4$, Sn_2Bu_6, toluene, 115 °C, 48 h, 83 %; c) $MeNH_2$ (33 % in EtOH), 60 °C, 2 h, 94 %; d) maleic anhydride, Et_2O, rt, 2 h, then acetic anhydride, KOAc, 90 °C, 2 h, 30 %.

tography standard was performed according to Scheme 2. 4-Iodophenethylamine was reacted with malemide to yield *N*-[4-iodophenethyl]-maleimide (**9**) in 38 % yield.

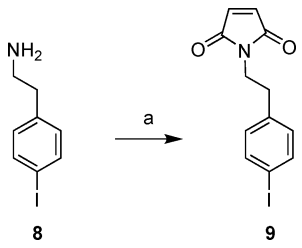

Scheme 2. *Reagents and conditions*: a) maleic anhydride, Et_2O, rt, 2 h, then acetic anhydride, KOAc, 90 °C, 2 h, 38 %.

Radioiodination of 7

Precursor **7** was radioiodinated using Chloramine-T as an oxidant (Scheme 3). As our goal was "one-pot" labeling, that is, performing radioiodination of a precursor and conjugation of radio-IPEM to prereduced Affibody molecules without intermediate purification, we tried to determine a minimum amount of **7** that provides a stable high yield. In the first series

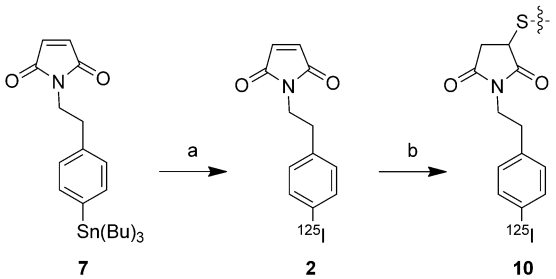

Scheme 3. *Reagents and conditions*: a) $^{125}I^-$, Chloramine-T, MeOH/HOAc, rt; b) $Z_{HER2:2395}$-Cys; pH 6.3.

of labeling experiments, the amount of **7** dissolved in ethanol was varied, while the amount of oxidant was constant (40 μg, ~140 nmol) and reaction time was 10 min. The influence of the amount of **7** on labeling yield is shown in Figure 2. Between

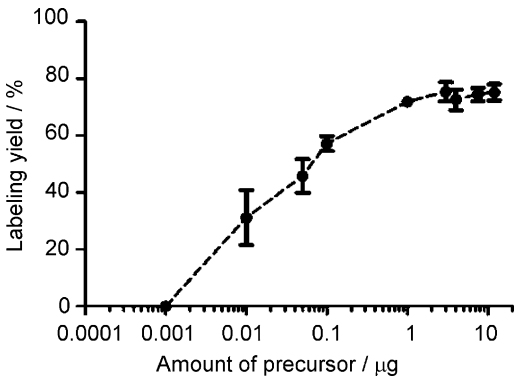

Figure 2. Dependence of radioiodination yield on the amount of the precursor **7**. Note the logarithmic scale. *Reagents and conditions*: CAT (40 μg), reaction time 10 min. Data are presented as mean ± maximum error ($n=2$).

0.01 μg (0.02 nmol) to 1 μg (2 nmol) the labeling yield increased proportionally with the amount of added precursor, from 31 ± 10 % up to 71.9 ± 0.4 %. An additional amount of precursor up to 12 μg (~24 nmol) did not further improve the labeling yield significantly. In a blank experiment where only solvent (5 % acetic acid in methanol) was used, no labeling yield could be determined (Figure 3).

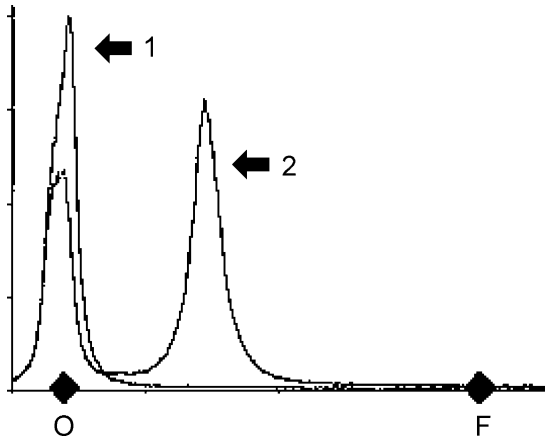

Figure 3. Distribution of radioactivity on a TLC plate. Origin (O) and solvent front (F) are marked. 1) Blank experiment (no precursor **7** is added). The only peak is at $R_f=0$, which is the same R_f as cold iodide. 2) Analysis of a typical reaction mixture after quenching. An additional radioactivity peak appears with $R_f=0.4$, as cold **9**.

Iododestannylation of **7** was apparently rapid (Figure 4). When 3 μg (6 nmol) of **7** was used, a yield of 73 ± 3 % was obtained already after 1 min, and further prolongation of the reaction time did not increase the yield significantly.

For further labeling experiments, the following conditions were selected: 2 μg (4 nmol) of **7**, 40 μg (140 nmol) of Chloramine-T, and a reaction time of 2 min.

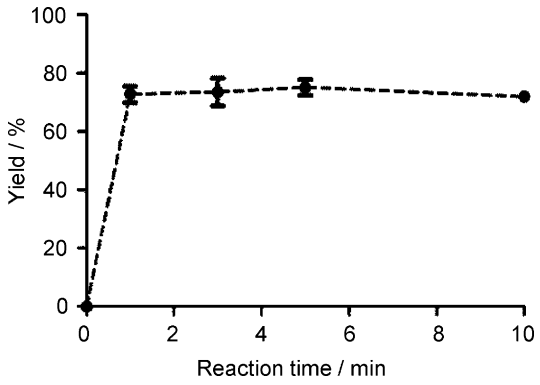

Figure 4. Dependence of radioiodination yield on reaction time. *Reagents and conditions*: CAT (40 μg), precursor **7** (3 μg). Data are presented as mean ± maximum error ($n = 2$).

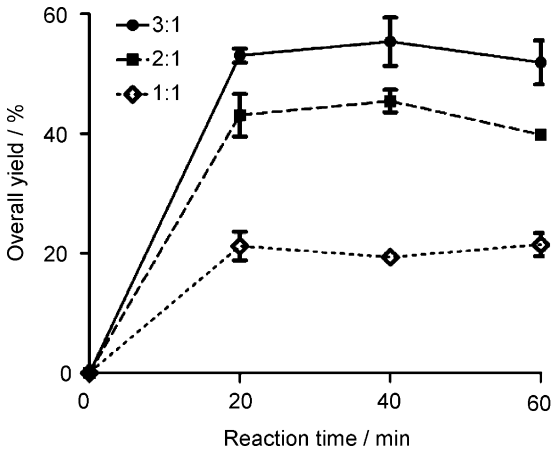

Figure 5. Overall radiochemical yield of labeling of $Z_{HER2:2395}$ after coupling with ^{125}I-IPEM. *Reagents and conditions*: 0.2 M NH_4OAc, pH 6.3, rt. Affibody:precursor molar ratios were 1:1, 2:1, and 3:1. Data are presented as mean ± maximum error ($n = 2$).

Conjugation of IPEM (8) to $Z_{HER2:2395}$

The conjugation of ^{125}I-IPEM to a prereduced $Z_{HER2:2395}$ was performed using a one-pot two-step approach, that is, in the same reaction vial as iododestannylation without purification of **2**. The coupling yield of ^{125}I-IPEM to $Z_{HER2:2395}$ was measured by varying Affibody:IPEM molar ratios (1:1, 2:1, and 3:1). The samples were analyzed at 20, 40, and 60 min. The overall labeling yield (i.e. incorporation of radioiodine into Affibody molecules) after 20 min incubation was 21 ± 2% and 43 ± 4% for Affibody:IPEM ratios of 1:1 and 2:1, respectively. The highest overall yield, 53 ± 1%, was obtained at the ratio of 3:1 (Figure 5). Since the difference between ratios 2:1 and 3:1 was small, the ratio of 2:1 was used for preparation of conjugates for in vivo and in vitro experiments in order to keep a higher specific activity of the conjugate. Given that the yield remained reasonably constant for the three time points, the incubation time was set to 40 min. According to instant thin-layer chromatography (ITLC) analysis, purification of ^{125}I-IPEM-$Z_{HER2:2395}$ using a NAP-5 size-exclusion column provided a radiochemical purity of 98.9 ± 0.5%.

The radioiodination of ^{125}I-IHPEM-$Z_{HER2:2395}$ resulted in an overall labeling yield of 45 ± 3% at an Affibody:HPEM molar ratio of 2:1 and a radiochemical purity of 99% after separation on an NAP-5 size exclusion column.

Stability test

To ensure that radioiodine is attached to the Affibody molecules via a stable covalent bond, samples of ^{125}I-IPEM-$Z_{HER2:2395}$ were incubated up to 4 h in 2 M of sodium iodide to replace noncovalently bound ^{125}I and in 30% ethanol to displace a noncovalently bound **2**. Incubation in sodium iodide resulted in a radiochemical purity of 98.5 ± 0.1%, and incubation in 30% ethanol in a purity of 99.4 ± 0.1%. The purity of control samples, which were kept in phosphate-buffered saline (PBS) was 99.4 ± 0.1%, that is, the difference was within experimental accuracy. Keeping samples in PBS for 24 h at 4 °C and 37 °C resulted in a purity of 97.3 ± 2.1% and 99.3 ± 0.3%, respectively.

In vitro studies

To verify that the binding of the labeled $Z_{HER2:2395}$ was specific to HER2 receptors, the labeled Affibody conjugates were incubated with a HER2-overexpressing human ovarian carcinoma cell line (SKOV-3) presaturated with nonlabeled $Z_{HER2:2395}$. Saturation of HER2 caused significant ($p < 0.00005$) decrease of cell-bound activity, from 53.7 ± 0.9% to 2.6 ± 0.1% for ^{125}I-IPEM-$Z_{HER2:2395}$ and from 56.8 ± 0.8% to 2.8 ± 0.1% for ^{125}I-IHPEM-$Z_{HER2:2395}$(Figure 6). This demonstrates that the binding of the conjugates to HER2-expressing cells is saturable, which suggests its receptor specificity.

Data concerning binding and cellular processing of ^{125}I-IPEM-$Z_{HER2:2395}$ and ^{125}I-IHPEM-$Z_{HER2:2395}$ by HER2-expressing SKOV-3 cells are shown in Figure 7. The two compounds showed simi-

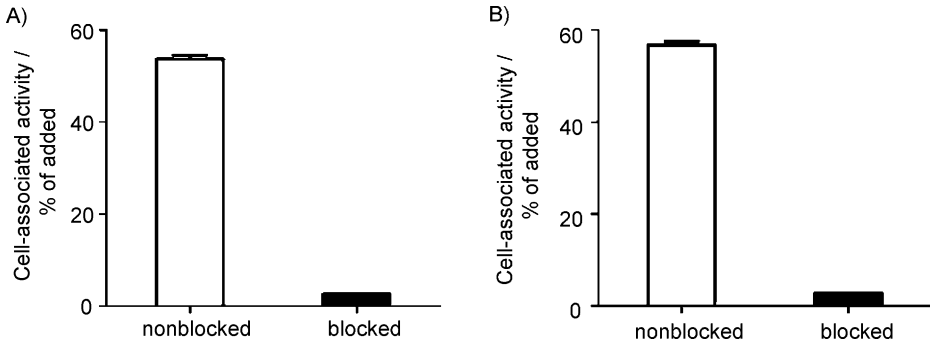

Figure 6. Binding specificity of ^{125}I-IPEM-$Z_{HER2:2395}$ (A) and ^{125}I-IHPEM-$Z_{HER2:2395}$ (B) to HER2-expressing SKOV-3 cells. Two groups of culture dishes containing SKOV-3 cells were incubated with radiolabeled conjugate (27 pM). One group of culture dishes was pretreated with saturating amounts of nonlabeled Affibody molecule (blocked). Cell-associated radioactivity was calculated as a percentage of total added radioactivity. Data are presented as mean value ± S.D. ($n = 3$).

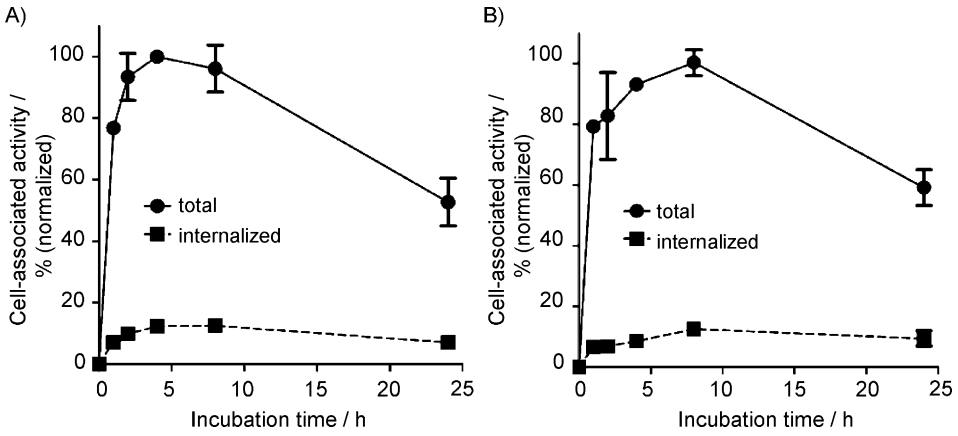

Figure 7. Binding and cellular processing of ^{125}I-IPEM-$Z_{HER2:2395}$ (A) and ^{125}I-IHPEM-$Z_{HER2:2395}$ (B) by HER2-expressing SKOV-3 cells. Conjugates (27 pM) were incubated at 37 °C. Acid wash was used to determine the membrane-bound radioactivity. Cell-bound activity is normalized to the maximum uptake. Data are presented as mean value ± S.D. ($n = 3$). Error bars might not be seen because they are smaller than the point symbols.

lar binding and processing patterns. A rapid increase in cell-associated activity was followed by a slower increase phase, a maximum, and then a decrease in cell-bound activity. The maximum value of cellular uptake was obtained at an earlier time point (4 h) by ^{125}I-IPEM-$Z_{HER2:2395}$ than by ^{125}I-IHPEM-$Z_{HER2:2395}$ (8 h). The level of internalized radioactivity was low (below 10%) during whole observation period for both conjugates.

Biodistribution study in mice

Comparison of ^{125}I-IPEM-$Z_{HER2:2395}$ and ^{125}I-IHPEM-$Z_{HER2:2395}$ biodistribution in NMRI mice is shown in Table 1 and Figure 8. A common feature of both variants was rapid clearance from blood (less than 3% injected activity (IA) g^{-1} at 1 h and less than 1% IA g^{-1} at 4 h postinjection (pi)). It has to be noted that blood concentration was significantly ($p < 0.05$) lower for ^{125}I-IHPEM-$Z_{HER2:2395}$ at all time points. Clearance from other organs and tissues was also rapid. Importantly, the renal uptake of ^{125}I-IPEM-$Z_{HER2:2395}$ (24 ± 2% and 5.7 ± 0.3% IA g^{-1} at 1 h and 4 h pi, respectively) were significantly ($p < 0.05$) lower than the uptake of ^{125}I-IHPEM-$Z_{HER2:2395}$ (50 ± 8% and 12 ± 2% IA g^{-1} at 1 h and 4 h pi, respectively). This confirms the main hypothesis that the use of a more hydrophobic linker decreases the retention of radioiodine in kidney after injection of Affibody molecules. Organs expressing Na^+/I^- symporter, that is, the stomach and salivary gland, showed a significantly ($p < 0.05$) lower radioactivity uptake in the case of ^{125}I-IPEM-$Z_{HER2:2395}$ in at least one time point. Although ^{125}I-IPEM-$Z_{HER2:2395}$ had higher uptake in liver at 1 h pi (4.1 ± 0.7% IA g^{-1} compared to 2.6 ± 0.1% IA g^{-1} for ^{125}I-IHPEM-$Z_{HER2:2395}$), the difference disappeared by 4 h pi (1.4% IA g^{-1} for both conjugates). Of note is the significantly higher radioactivity in the gastrointestinal tract (with content) for ^{125}I-IHPEM-$Z_{HER2:2395}$, which indicates that a larger fraction of this conjugate or its radiometabolites is excreted via bile.

Table 1. Comparison of the biodistribution of ^{125}I-IPEM-$Z_{HER2:2395}$ and ^{125}I-IHPEM-$Z_{HER2:2395}$ in NMRI mice.

	Uptake [% IA g^{-1}]					
	1 h		4 h		24 h	
	IPEM	IHPEM	IPEM	IHPEM	IPEM	IHPEM
Blood	2.8 ± 0.4[a]	2.2 ± 0.2	0.81 ± 0.06[a]	0.56 ± 0.04	0.38 ± 0.03[a]	0.12 ± 0.07
Lung	2.8 ± 0.5	2.6 ± 0.3	0.57 ± 0.04	0.54 ± 0.06	0.13 ± 0.01[a]	0.07 ± 0.01
Liver	4.1 ± 0.7[a]	2.7 ± 0.1	1.4 ± 0.1	1.4 ± 0.3	0.18 ± 0.06[a]	0.07 ± 0.02
Spleen	1.0 ± 0.2	0.9 ± 0.1	0.34 ± 0.04	0.29 ± 0.05	0.12 ± 0.01[a]	0.04 ± 0.03
Stomach	1.1 ± 0.1[a]	2.1 ± 0.4	0.40 ± 0.05[a]	2 ± 1	0.05 ± 00.01	0.07 ± 0.03
Kidney	24 ± 2[a]	50 ± 9	5.7 ± 0.3[a]	12 ± 2	0.90 ± 0.09[a]	0.6 ± 0.3
Salivary gland	1.0 ± 0.2	1.2 ± 0.6	0.34 ± 0.06[a]	1.6 ± 0.3	0.026 ± 0.008	0.040 ± 0.003
Muscle	0.6 ± 0.1	1.1 ± 0.9	0.11 ± 0.01	0.12 ± 0.04	0.012 ± 0.003	0.010 ± 0.002
GI tract[b]	9 ± 1[a]	12 ± 1	9.8 ± 0.9[a]	18 ± 3	0.18 ± 0.04	0.32 ± 0.09
Carcass	14 ± 2	14 ± 1	3.1 ± 0.3	3.8 ± 1.0	0.57 ± 0.09	1.18 ± 0.66

[a] Significant ($p < 0.05$) difference between ^{125}I-IPEM-$Z_{HER2:2395}$ and ^{125}I-IHPEM-$Z_{HER2:2395}$ at the same time point. [b] Data from gastrointestinal (GI) tract with content and carcass are presented as % of injected radioactivity per whole sample. Data are presented as mean ± S.D. ($n = 4$ mice).

Discussion

Engineered scaffold proteins such as Affibody molecules, are an emerging alternative to Mabs in radionuclide tumor targeting for diagnostics and therapy. A precondition for successful clinical application of scaffold proteins is maximizing the delivery and retention of radionuclides in tumors and minimizing their delivery and retention in normal tissues. In the case of imaging, this provides higher contrast and, therefore, sensitivity. In the case of radionuclide therapy, this ensures destruction of tumors while sparing normal tissues. Hence, a decrease in uptake and retention of radionuclides in normal tissues is as important as an increase in tumor uptake. This study focused on the decrease of renal radioactivity delivered by Affibody molecules.

The decrease in renal radioactivity might be achieved, in principle, by the decrease in renal reabsorption of targeting proteins or by the decrease in retention of radiocatabolites in proximal tubuli cells. Previous studies[31] have demonstrated that the scavenger receptor megalin is not involved in renal reabsorption of Affibody molecules. Therefore, common methods for the decrease in renal reabsorption of small proteins and peptides in kidneys, e.g. saturation

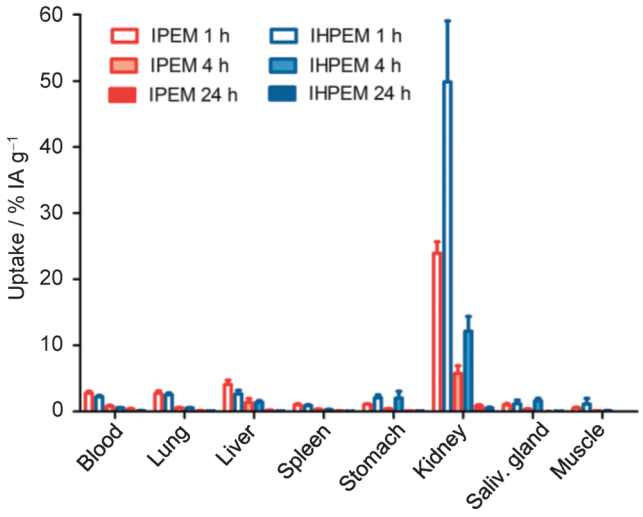

Figure 8. Comparison of biodistribution of ^{125}I-IPEM-$Z_{HER2:2395}$ and ^{125}I-IHPEM-$Z_{HER2:2395}$ in NMRI mice. The uptake is expressed as % IA g^{-1}, and presented as mean ± S.D. (n = 4 mice).

of scavenger receptors by co- or preinjection of cationic amino acids or Gelofusine, do not work. Therefore, minimization of retention of radiocatabolites in proximal tubuli is the only viable alternative at the moment. Our previous studies have demonstrated that this goal might be achieved for both radiohalogens[25,27] and for such radiometals as ^{99m}Tc[32,33] and radioisotopes of rhenium.[34,35] It has to be admitted that such decrease was achieved as a result of structure–property relationship studies, and molecular and biological mechanisms leading to this are still not quite clear for us. This study should elucidate the effect of lipophilicity of a prosthetic group, used in the attachment of a radiohalogen to an Affibody molecule, on renal retention.

Synthesis of ^{125}I-IPEM for the labeling of Fab fragments was reported by Hylarides and co-workers in 1991.[30] Factors influencing labeling efficiency were described in the initial report. Unfortunately, we did not find any follow-up studies concerning this interesting precursor for radioiodination. ^{125}I-IPEM attracted our attention because it is suitable for thiol-directed site-specific labeling of cysteine-containing Affibody molecules and its hydrophobicity ($\log P = 2.85$) is higher than that of ^{125}I-IHPEM ($\log P = 2.46$).

Iododestannylation of **7** was efficient, enabling a yield in excess of 70% when 1–3 μg (2–6 nmol) was used for labeling (Figure 2). The reaction was rapid, and the high yield was achieved within 1 min (Figure 4), when 3 μg of **7** was used. The efficient labeling of a small amount of precursor removed the need for the intermediate purification of **2**, i.e. we can perform the whole conjugation "in one pot". This approach minimizes the handling of radioactive compounds, the associated dose burden to personnel, the losses during transfer of labeled precursor, and the probability of human error.[36] The overall labeling yield of the two-step process was a modest ~20% when an Affibody:precursor molar ratio of 1:1 was used (Figure 5). Increasing the ratio to 2:1 doubled the overall yield, but a further increase in relative protein amount was relatively inefficient. The Affibody:precursor ratio of 2:1 was selected for further labeling to keep a reasonably high specific activity. The conjugation time of 20–30 min was sufficient to reach the maximum overall yield (Figure 5). Importantly, the binding of ^{125}I-IPEM-$Z_{HER2:2395}$ to HER2-expressing SKOV-3 cells was saturable (Figure 5A), which demonstrates that the binding specificity of the Affibody molecule was preserved after labeling. Binding specificity of the alternative, ^{125}I-IHPEM-$Z_{HER2:2395}$, has also been confirmed (Figure 5B).

The internalization rate of anti-HER2 Affibody molecules by cancer cells is rather slow and reaches 30–40% per day in the case of residualizing labels.[27] This internalization rate corresponds to daily cell-surface renewal. In this study the internalized fraction of radioactivity was below 10% at all time points which reflects nonresidualizing properties of radiocatabolites. After binding to a cell-surface receptor, a fraction of Affibody molecules is internalized, transferred to the lysosomal compartment, and degraded by proteolytic enzymes. Lipophilic radiometabolites diffuse through lysosomal and cellular membranes and leak out from cells. A maximum cell-associated activity is achieved when the binding rate is equal to the rate of radiocatabolite leakage. In the case of a higher leakage rate, the maximum is reached earlier. A comparison of binding to SKOV-3 cells (Figure 7) shows that the maximum cell-associated activity for ^{125}I-IPEM-$Z_{HER2:2395}$ was reached earlier (4 h) than for ^{125}I-IHPEM-$Z_{HER2:2395}$ (8 h). This suggests that ^{125}I-IPEM provides more "leaky" radiometabolites. It has to be noted that internalization of anti-HER2 Affibody molecules by cancer cells is rather slow,[20,21,28] and the difference is therefore relatively small. This complicates in vitro evaluation of an internalization rate, but is favorable for in vivo tumor targeting, as leakage of radiocatabolites has a small effect on tumor-associated radioactivity.[37] On the other hand, the internalization rate in kidneys is high, and the difference in radiocatabolite leakage rate has to be much more pronounced.

Direct in vivo comparison of ^{125}I-IPEM-$Z_{HER2:2395}$ and ^{125}I-IHPEM-$Z_{HER2:2395}$ biodistribution in NMRI mice confirmed the main hypothesis of this study (Table 1). The renal radioactivity was two times lower for ^{125}I-IPEM-$Z_{HER2:2395}$ than for ^{125}I-IHPEM-$Z_{HER2:2395}$ at 1 h and 4 h after injection. It has to be noted that the label nature has a clear influence in uptake in other organs. For example, hepatic uptake of ^{125}I-IPEM-$Z_{HER2:2395}$ (4.1 ± 0.7% IA g^{-1}) at 1 h pi was significantly higher than uptake of ^{125}I-IHPEM-$Z_{HER2:2395}$ (2.7 ± 0.1% IA g^{-1}). This might be because of the higher overall lipophilicity of ^{125}I-IPEM-$Z_{HER2:2395}$, as higher lipophilicity is generally associated with higher liver uptake.[38] However, the difference disappeared at 4 h pi, a time point relevant for imaging. More disturbing was the 1.5-fold higher blood level of ^{125}I-IPEM-$Z_{HER2:2395}$, as this could negatively affect imaging contrast. This phenomenon might be associated with the release of radiometabolites from kidneys to blood or with higher adhesion to blood proteins. Another interesting feature of ^{125}I-IPEM-$Z_{HER2:2395}$ was lower radioactivity uptake in the stomach and salivary gland. As both these organs express the Na^+/I^-symporter, it is likely that the metabolism of ^{125}I-IPEM results in the decreased release of free radioiodide. Overall, this

study demonstrated the very pronounced influence of a prosthetic group for radioiodination on the distribution of radioactivity after injection of Affibody molecules.

This information might also be helpful in the development of other imaging probes based on engineered scaffold proteins. It has to be noted that this approach is justified when internalization of an imaging agent by cancer cells is slow but internalization by tubuli cells is rapid. In the case of rapid internalization by cancer cells, the use of a prosthetic group providing lipophilic radiometabolites would decrease tumor accumulation of radioactivity. In this case, radioiodination using prosthetic groups providing charged radiometabolites would be recommended.[39]

Conclusions

The use of a more lipophilic radioiodine label at the C-terminus of Affibody molecules is associated with lower renal retention of radioactivity. This suggests that a careful selection of the labeling strategy could be used in the modification and optimization of the biodistribution profile of radiohalogenated imaging agents.

Experimental Section

Materials

^{125}I was purchased from PerkinElmer (Waltham, USA). Organic solvents were purchased from Merck (Darmstadt, Germany). Chloramine-T (CAT) and $Na_2S_2O_5$ were from Sigma (St. Louis, USA). Buffers, including 0.1 M PBS (pH 7.5) and 0.2 M NH_4OAc (pH 6.3), were prepared using common methods from chemicals supplied by Merck (Darmstadt, Germany). High-quality Milli-Q water (resistance higher than 18 MΩ cm) was used for preparing the solutions and buffers. Solutions of CAT, $Na_2S_2O_5$, iodophenethylmaleimide, and hydroxylphenethylmaleimide were prepared immediately before use. TLC plates were developed in 1,2-dichlorethane (BDH chemicals, Poole Dorset, UK) followed by heating. Distribution of radioactivity along the TLC plates and ITLC strips was measured using a Cyclone Storage phosphor system and analyzed with the OptiQuant image analysis software (PerkinElmer, Waltham, USA). The radiochemical purity of the labeled Affibody molecule construct was analyzed using 150–771 DARK GREEN, Tec-control Chromatography Strips (ITLC) from Biodes medical system (New York, USA). Size-exclusion chromatography was performed on disposable NAP-5 columns (Amersham Pharmacia Biotech AB, Uppsala, Sweden) according to the manufacturer's instructions.

Cellular experiments were performed using human ovarian carcinoma cells, SKOV-3 (ATCC, purchased via LGCPromochem, Borås, Sweden). Ketalar (ketamine, 50 mg mL^{-1}, Pfizer, New York, USA), Rompun (xylazin, 20 mg mL^{-1}, Bayer, Leverkusen, Germany), and heparin (5000 IE mL^{-1}, Leo Pharma, Copenhagen, Denmark) were obtained commercially.

NMR spectra were recorded on a Varian Mercury Plus spectrometer (Santa Clara, USA) at ambient temperature. Chemical shifts are referenced via the residual solvent signals (^{1}H: $CHCl_3$ at 7.26 ppm; ^{13}C: $CDCl_3$ at 77.16 ppm). TLC was carried out on Merck precoated 60 F254 aluminum plates (0.2 mm) using UV light (254 nm). Charring with 8% phosphomolybdic acid (PMA) in absolute EtOH or 0.5% ninhydrine in EtOH (95%) was used for visualization. Flash column chromatography was performed using silica gel 60 (0.040–0.063 mm, Merck). Analytical liquid chromatography/mass spectrometry (LC-MS) was performed on a Gilson HPLC system with a Finnigan AQA-quadropole mass spectrometer (Gilson Inc., Middleton, USA) using a C18 (5 μm, 4.6×100 mm) column, with a 5 min gradient of 60–100% CH_3CN in 0.05% aq HCOOH as mobile phase at a flow rate of 4 mL min^{-1}. All starting materials and reagents were purchased from Sigma–Aldrich Sweden (Stockholm) and used without further purification. All synthesized molecules are >95% pure as shown by TLC, analytical LC-MS, and NMR spectroscopy. The radioactivity was measured using an automated gamma counter with a 1480 Wizard three-inch NaI (Tl) detector (Wallac Oy, Turku, Finland). The production of $Z_{HER2:2395}$ was described earlier.[20]

Synthesis of *N*-(4-bromophenethyl)phthalimide (4)

To a stirred solution of **3** (1.0 g, 5 mmol in 50 mL diethyl ether) was added phthalic anhydride (741 mg, 5 mmol). The mixture was stirred for 2 h. Afterwards, a white precipitate (carbamoylbenzoic acid) was collected after filtration and washed with cold diethyl ether (3 ×30 mL). The acid was dissolved in glacial CH_3COOH (15 mL) and heated at 65 °C for 3 h. The mixture was cooled to rt and was allowed to precipitate overnight. Filtration and washing with cold CH_3COOH (3×20 mL) provided **4** as a white powder (81%, 1.33 g); ^{1}H NMR (400 MHz, 25 °C, $CDCl_3$): δ = 7.86–7.83 (m, 2H), 7.73–7.71 (m, 2H), 7.41–7.39 (m, 2H), 7.14–7.12 (m, 2H), 3.93–3.89 (m, 2H), 2.98–2.94 ppm (m, 2H); ^{13}C NMR (100 MHz, 25 °C, $CDCl_3$): δ = 168.1, 136.9, 134.0, 131.6, 132.0, 130.6, 123.3, 120.5, 38.9, 34.0 ppm; MS (ESI): 330–332 [$M+H^+$].

Synthesis of *N*-[(tri-*n*-butylstannyl)phenethyl]phthalamide (5)

A pressure-resistant 50 mL glass tube was loaded with **4** (500 mg, 1.5 mmol), bis(tributyltin) (2.63 g, 4.5 mmol, 3 equiv), tetrakis(triphenylphosphine)palladium(0) (35 mg, 0.03 mmol, 2 mol%), and anhydrous toluene (15 mL). The tube was flushed with nitrogen and, after capping, heated at 115 °C for 48 h. After cooling to rt, the crude dark mixture was evaporated and purified by column chromatography yielding compound **5** as a clear viscous oil (83%, 675 mg): R_f = 0.2 (isohexane/EtOAc 9:1); ^{1}H NMR (400 MHz, 25 °C, $CDCl_3$): δ = 7.85–7.64 (m, 4H), 7.44–7.32 (m, 2H), 7.26–7.20 (m, 2H), 3.94–3.89 (m, 2H), 2.99–2.93 (m, 2H), 1.65–1.25 (m, 12H), 1.10–0.98 (m, 6H), 0.92–0.80 ppm (m, 9H); ^{13}C NMR (100 MHz, 25 °C, $CDCl_3$): δ = 168.2, 139.8, 137.6, 136.7, 133.9, 132.1, 128.5, 123.2, 39.2, 34.6, 29.0, 27.4, 13.7, 9.5 ppm; ESI (MS): 537–545 [$M+H^+$].

Synthesis of 4-tri-*n*-butylstannylphenethylamine (6)

To a pressure-resistant 50 mL glass tube containing **5** (600 mg, 1.1 mmol), CH_3NH_2 (10 mL, 33% in absolute EtOH) was added. The tube was capped and heated to 60 °C for 2 h. After cooling, the solvent was removed leaving a white solid. NaOH (20 mL, 2.5 M) was added and then extracted with diethyl ether (3×30 mL). The organic phases were combined, dried over $MgSO_4$, and evaporated leaving the desired product,[2] compound **6**, as a clear low viscous oil (94%, 426 mg); ^{1}H NMR (400 MHz, 25 °C, $CDCl_3$): δ = 7.39 (t, J = 7.8 Hz, 2H), 7.17 (t, J = 7.8 Hz, 2H), 2.97 (t, J = 7.0 Hz, 2H), 2.73 (t, J = 7.0 Hz, 2H), 1.64–1.26 (m, 12H), 1.16–0.84 ppm (m, 15H); ^{13}C NMR (100 MHz, 25 °C, $CDCl_3$): δ = 139.5, 139.1, 136.6, 128.5, 43.5, 40.2, 29.0, 27.4, 13.7, 9.5 ppm; MS (ESI): 408–416 [$M+H^+$].

Synthesis of *N*-[(4-tri-*n*-butylstannyl)phenethyl]maleimide (7)

Compound **6** (400 mg, 0.98 mmol) was dissolved in diethyl ether (25 mL) where, after, maleic anhydride (115 mg, 1.2 mmol,

1.2 equiv) was added, and the reaction was left stirring for 2 h yielding crude maleanilinic acid. After removal of solvent in vacuo, acetic anhydride (30 mL) was added together with KOAc (295 mg, 3 mmol). The reaction was stirred at 90 °C for 2 h and then cooled to rt. To the mixture was added diethyl ether (30 mL) and then washed with H_2O (3×30 mL) and aq Na_2CO_3 (1×100 mL, 5%). The organic phase was then dried with $MgSO_4$, evaporated, and purified with column chromatography providing compound **7** as a clear viscous oil (30%, 140 mg): R_f=0.2 (isohexane:EtOAc:Et_3N 20:1:0.2); ^{1}H NMR (400 MHz, 25 °C, $CDCl_3$): δ=7.38 (t, J=7.8 Hz, 2H), 7.17 (t, J=7.8 Hz, 2H), 6.66 (s, 2H), 3.78–3.72 (m, 2H), 2.90–2.85 (m, 2H), 1.61–1.27 (m, 12H), 1.12–0.86 ppm (m, 15H); ^{13}C NMR (100 MHz, 25 °C, $CDCl_3$): δ=170.5, 139.9, 136.7, 134.0, 128.4, 39.1, 34.5, 29.0, 27.4, 13.7, 9.5 ppm; MS (ESI): 487–495 [$M+H^+$].

Synthesis of *N*-[4-iodophenethyl]-maleimide (9)

To a stirred solution of **8** (124 mg, 0.5 mmol) in diethyl ether (10 mL), maleic anhydride (57 mg, 0.6 mmol, 1.2 equiv) was added, and the reaction was left stirring for 2 h. The precipitate was collected and dissolved in glacial CH_3COOH (10 mL) and heated at 65 °C for 3 h. The mixture was cooled to rt and was allowed to precipitate overnight. The precipitate was filtered and washed with cold CH_3COOH (3×10 mL) resulting in compound **9** as a white powder (38%, 62 mg); ^{1}H NMR (400 MHz, 25 °C, $CDCl_3$): δ=7.61 (d, J=8.3 Hz, 1H), 7.19 (d, J=5.6 Hz, 1H), 6.99 (d, J=8.0 Hz, 1H), 6.59 (d, J=5.6 Hz, 1H), 3.87 (t, J=7.2 Hz, 1H), 2.92 ppm (t, J=7.2 Hz, 1H);^{13}C NMR (100 MHz, 25 °C, $CDCl_3$): δ=166.7, 142.2, 139.1, 137.6, 134.2, 131.0, 128.8, 91.7, 50.8, 36.3 ppm; MS (ESI): 378 [$M+H^+$].

Radioiodination of iodophenethylmaleimide (IPEM)

The precursor was radioiodinated using CAT as an oxidant. Typically ^{125}I (10 μL, 1 MBq μL^{-1}) was added to the precursor **7** (3 μL, dissolved in EtOH at a predetermined concentration) and solvent (10 μL, 5% HOAc in MeOH). To the mixture, CAT (10 μL, 4 μg μL^{-1} in Milli-Q H_2O) was added. The reaction proceeded for a predetermined time and then quenched by a double molar excess of $Na_2S_2O_5$ (6 μg μL^{-1} in Milli-Q H_2O).

The dependence of labeling yield on the amount of precursor and reaction time was determined by varying one parameter at a time. The amount of **7** varied between 0.01–15 μg and the reaction time varied between 1–10 min. When the amount of **7** varied, the reaction time was set at 10 min. When the reaction time was varied, the amount of **7** remained constant (3 μg).

Silica gel 60 F254 TLC plates (20×100 mm, elution path 80 mm) (Merck) were used for analysis. As eluent,1,2-dichlorethane was used. In this system, iodide remains at the origin while IPEM has an R_f of 0.4. The reaction mixture (1.8–2 μL) was applied to the ITLC plate, which was then left to evaporate spontaneously before being developed in the eluent. All experiments were done at least in duplicate. Blank experiments were performed where 5% HOAc in MeOH (3 μL) was used instead of **7**.

Conjugation of IPEM (2) to prereduced $Z_{HER2:2395}$

Before labeling, the Affibody molecule solution in PBS was treated with dithiothreitol (DTT, Merck) in order to reduce spontaneously formed disulfide bonds. Typically, the stock Affibody solution (50 μL, 10 μg μL^{-1}) in PBS was mixed with DTT (350 μL) in PBS to get a final concentration of 50 mM DTT. The mixture was incubated at 40 °C for 3 h at rt. Thereafter the mixture was applied to NAP-5 size-exclusion columns, pre-equilibrated, and eluted with well-degassed 0.2 M NH_4OAc (pH 6.3), containing 0.04 M sodium ascorbate. The first 900 μL of the high molecular weight (HMW) fraction was used for labeling. The reduced Affibody was used for labeling approximately 10–15 min after reduction. Compound **7** was radioiodinated as described above. To get the best conjugation conditions, the Affibody:IPEM molar ratio was varied between 1:1, 2:1, and 3:1. $Z_{HER2:2395}$ was added in varying amounts to the ^{125}I-IPEM solution (2 μg of **7**) and incubated at rt. Small fractions (~1.5 μL) were analyzed on ITLC silica gel strips developed in 80% acetone in H_2O, at 20, 40, and 60 min. In this system, the Affibody molecule remains at the origin, and IPEM and iodide have an R_f of 1.0. After conjugation, ^{125}I-IPEM-$Z_{HER2:2395}$was purified using an NAP-5 size-exclusion column pre-equilibrated with PBS. The mixture (1.6 μL) was analyzed using radio-ITLC to determine radiochemical purity of the final product. All experiments were done in duplicate.

Stability test

The stability of radioiodine coupling to the $Z_{HER2:2395}$was assessed by incubating the solution for at 4 °C for 24 h and thereafter at rt for 4 h. Stability was further analyzed by incubating the radioiodinated $Z_{HER2:2395}$with 2 M NaI or 30% EtOH, both for 1 h. The labeling was done as described above and purified via NAP-5 size-exclusion chromatography. ^{125}I-IPEM-$Z_{HER2:2395}$ was added in equal volume (50 μL) to Eppendorf tubes containing 2 M NaI in PBS, and the solution was incubated for 1 h. For the stability test in EtOH, 95% EtOH (30 μL) was added to the sample (70 μL) in Eppendorf tubes, and the solution was incubated for 1 h. All experiments were done in duplicate and analyzed using ITLC strips.

Labeling of HPEM

Labeling of HPEM was performed as previously described.[26] In brief, HPEM precursor solution(5 μg) in 5% HOAc in MeOH was mixed with ^{125}I (10 μL). To the mixture, aq CAT solution (10 μL, 4 μg μL^{-1}) was added, and the solution was incubated for 5 min. The reaction was terminated by adding aq $Na_2S_2O_5$ (10 μL, 6 μg uL^{-1}), given in double molar excess to CAT. Conjugations of ^{125}I-IHPEM (**1**) to $Z_{HER2:2395}$was done as described for ^{125}I-IPEM with an Affibody/HPEM molar ratio of 2:1.

Binding specificity and cellular processing of labeled conjugates to HER2-expressing cells

The binding specificity of the ^{125}I-IPEM- and ^{125}I-IHPEM-$Z_{HER2:2395}$ conjugates to HER2 were evaluated using HER2-expressing SKOV-3 ovarian cancer cells as previously described.[27] Briefly, a solution of ^{125}I-IPEM-$Z_{HER2:2395}$ or ^{125}I-IHPEM-$Z_{HER2:2395}$ (1.99 ng/dish, 27 pM) was added to a set of two groups of petri dishes (1×10^6 cells/dish). To block the receptors, an excess of nonlabeled $Z_{HER2:2395}$was added 5 min before applying the labeled conjugate to one group of dishes. The cells were incubated in 37 °C for 1 h in a humidified incubator; thereafter, the cell media was collected, and the cells were detached with trypsin-EDTA solution (0.5 mL, 0.5% trypsin, 0.02% EDTA in buffer, Biochrom AG, Berlin, Germany). Then the complete medium (0.5 mL) was added to every dish, and cells were resuspended and collected. The percentage of cell-bound radioactivity was calculated by measuring the radioactivity in the media and the cells.

Processing of ^{125}I-IPEM-$Z_{HER2:2395}$ and ^{125}I-IHPEM-$Z_{HER2:2395}$ by SKOV-3 cells was studied according to a method previously described and validated.[27] The labeled compounds (1.99 ng/dish, 27 pM) were added to each dish, with three dishes per time point per conjugate (1×10^6 cells/dish). The cells were incubated at 37 °C, 5% CO_2. At predetermined time points (1, 2, 4, 8, and 24 h after the start of incubation), the media from the dishes was collected, and the cells were washed with ice-cold serum-free medium. The cells were then treated with 0.2 M glycine buffer containing 4 M urea, pH 2.5,

(0.5 mL) for 5 min on ice. The solution was collected, and the cells were washed additionally with glycine buffer (0.5 mL), the fractions were pooled together. The radioactivity from the acid wash fractions was considered to be membrane bound. The cells were then incubated at 37 °C for at least 30 min with 1 M NaOH (0.5 mL).The alkaline solution was collected, the cell dishes were washed with an additional NaOH (0.5 mL), and the alkaline fractions were pooled. The radioactivity in the alkaline fractions was considered internalized. The percent of internalized radioactivity was calculated for each fraction at each time point.

Biodistributions study in NMRI mice

All animal experiments were planned and performed according to the Swedish national legislation on the protection of laboratory animals, and the study plans were approved by the Uppsala committee for animal research ethics (Uppsala djurförsöksetiskanämd, permission C224/10 given to A. Orlova). Female NMRI mice (10–12 weeks old at arrival) were acclimatized for one week at the Rudbeck Laboratory animal facility. Groups of four animals per time point were used for the biodistribution study. Animals were intravenously injected with 30 kBq of either ^{125}I-PEM-$Z_{HER2:2395}$ (4 μg) or ^{125}I-HPEM- $Z_{HER2:2395}$ (4 μg) dissolved in PBS (100 μL). At 1 h, 4 h, and 24 h after injection, a mixture of Ketala-Rompun (20 μL solution per gram body weight, Ketalar: 10 mg mL^{-1}, Rompun: 1 mg mL^{-1}) was injected intraperitonealy. The mice were sacrificed by heart puncture. Blood was collected, and organ samples were excised. The samples were put in preweighed plastic vials. The samples were weighed, and their radioactivity was measured. The uptake in tissue and organ were calculated as percent injected activity per gram tissue (% IA g^{-1}). For the gastrointestinal tract and the carcass, injected activity per whole sample was calculated (% IA g^{-1}).

Acknowledgements

This research was financially supported by Swedish Cancer Society (Cancerfonden) and the Swedish Research Council (Vetenskapsradet).

Keywords: affibody molecules · drug design · iodophenethylmaleimide · radiolabeling · radiopharmaceuticals

[1] D. Hanahan, R. A. Weinberg, *Cell* **2011**, *144*, 646 – 674.
[2] B. Fauvel, A. Yasri, *MAbs.* **2014**, *6*, 838 – 851.
[3] V. Pillay, H. K. Gan, A. M. Scott, *New Biotechnol.* **2011**, *28*, 518 – 529.
[4] A. M. Wu, P. D. Senter, *Nat. Biotechnol.* **2005**, *23*, 1137 – 1146.
[5] S. E. Jackson, J. D. Chester, *Int. J. Cancer.* **2014**, DOI: 10.1002/ijc.28940.
[6] V. Tolmachev, S. Stone-Elander, A. Orlova, *Lancet Oncol.* **2010**, *11*, 992 – 1000.
[7] S. Heskamp, H. W. van Laarhoven, W. T. van der Graaf, W. J. Oyen, O. C. Boerman, *Expert Opin. Drug Delivery* **2014**, *11*, 175 – 185.
[8] D. M. Goldenberg, *J. Nucl. Med.* **2002**, *43*, 693 – 713.
[9] Z. Miao, J. Levi, Z. Cheng, *Amino Acids* **2011**, *41*, 1037 – 1047.
[10] P. A. Nygren, *FEBS J.* **2008**, *275*, 2668 – 2676.
[11] J. Löfblom, J. Feldwisch, V. Tolmachev, J. Carlsson, S. Ståhl, F. Y. Frejd, *FEBS Lett.* **2010**, *584*, 2670 – 2680.
[12] A. Orlova, M. Magnusson, T. L. Eriksson, M. Nilsson, B. Larsson, I. Höidén-Guthenberg, C. Widström, J. Carlsson, V. Tolmachev, S. Ståhl, F. Y. Nilsson, *Cancer Res.* **2006**, *66*, 4339 – 4348.
[13] V. Tolmachev, J. Malmberg, C. Hofström, L. Abrahmsén, T. Bergman, A. Sjöberg, M. Sandström, T. Gräslund, A. Orlova, *J. Nucl. Med.* **2012**, *53*, 90 – 97.
[14] J. Strand, Z. Varasteh, O. Eriksson, L. Abrahmsen, A. Orlova, V. Tolmachev, *Mol. Pharm.* **2014**, *11*, 3957 – 3964.
[15] V. Tolmachev, D. Rosik, H. Wållberg, A. Sjöberg, M. Sandström, M. Hansson, A. Wennborg, A. Orlova, *Eur. J. Med. Mol. Imaging* **2010**, *37*, 613 – 622.
[16] H. Honarvar, J. Garousi, E. Gunneriusson, I. Höidén-Guthenberg, M. Altai, C. Widström, V. Tolmachev, F. Y. Frejd, *Int. J. Oncol.* **2015**, *46*, 513 – 520.
[17] A. Orlova, H. Wållberg, S. Stone-Elander, V. Tolmachev, *J. Nucl. Med.* **2009**, *50*, 417 – 425.
[18] R. P. Baum, V. Prasad, D. Müller, C. Schuchardt, A. Orlova, A. Wennborg, V. Tolmachev, J. Feldwisch, *J. Nucl. Med.* **2010**, *51*, 892 – 897.
[19] J. Sörensen, D. Sandberg, M. Sandström, A. Wennborg, J. Feldwisch, V. Tolmachev, G. Åström, M. Lubberink, U. Garske-Román, J. Carlsson, H. Lindman, *J. Nucl. Med.* **2014**, *55*, 730 – 735.
[20] S. Ahlgren, A. Orlova, D. Rosik, M. Sandström, A. Sjöberg, B. Baastrup, O. Widmark, G. Fant, J. Feldwisch, V. Tolmachev, *Bioconjugate Chem.* **2008**, *19*, 235 – 243.
[21] J. Malmberg, A. Perols, Z. Varasteh, M. Altai, A. Braun, M. Sandström, U. Garske, V. Tolmachev, A. Orlova, A. E. Karlström, *Eur. J. Nucl. Med. Mol. Imaging* **2012**, *39*, 481 – 492.
[22] G. Kramer-Marek, D. O. Kiesewetter, L. Martiniova, E. Jagoda, S. B. Lee, J. Capala, *Eur. J. Nucl. Med. Mol. Imaging* **2008**, *35*, 1008 – 1018.
[23] M. Namavari, O. Padilla De Jesus, Z. Cheng, A. De, E. Kovacs, J. Levi, R. Zhang, J. K. Hoerner, H. Grade, F. A. Syud, S. S. Gambhir, *Mol. Imaging Biol.* **2008**, *10*, 177 – 181.
[24] D. Rosik, A. Thibblin, G. Antoni, H. Honarvar, J. Strand, R. K. Selvaraju, M. Altai, A. Orlova, A. Eriksson Karlström, V. Tolmachev, *Bioconjugate Chem.* **2014**, *25*, 82 – 92.
[25] E. Mume, A. Orlova, B. Larsson, A. S. Nilsson, F. Y. Nilsson, S. Sjöberg, V. Tolmachev, *Bioconjugate Chem.* **2005**, *16*, 1547 – 1555.
[26] V. Tolmachev, E. Mume, S. Sjöberg, F. Y. Frejd, A. Orlova, *Eur. J. Nucl. Med. Mol. Imaging* **2009**, *36*, 692 – 701.
[27] H. Wållberg, A. Orlova, *Cancer Biother. Radiopharm.* **2008**, *23*, 435 – 442.
[28] A. C. Steffen, M. Wikman, V. Tolmachev, G. P. Adams, F. Y. Nilsson, S. Ståhl, J. Carlsson, *Cancer Biother. Radiopharm.* **2005**, *20*, 239 – 248.
[29] V. Tolmachev, A. Orlova, H. Lundqvist, *Curr. Med. Chem.* **2003**, *10*, 2447 – 2460.
[30] M. D. Hylarides, D. S. Wilbur, M. W. Reed, S. W. Hadley, J. R. Schroeder, L. M. Grant, *Bioconjugate Chem.* **1991**, *2*, 435 – 440.
[31] M. Altai, Z. Varasteh, K. Andersson, A. Eek, O. Boerman, A. Orlova, *Cancer Biother. Radiopharm.* **2013**, *28*, 187 – 195.
[32] T. Ekblad, T. Tran, A. Orlova, C. Widström, J. Feldwisch, L. Abrahmsén, A. Wennborg, A. E. Karlström, V. Tolmachev, *Eur. J. Nucl. Med. Mol. Imaging* **2008**, *35*, 2245 – 2255.
[33] H. Wållberg, A. Orlova, M. Altai, S. J. Hosseinimehr, C. Widström, J. Malmberg, S. Ståhl, V. Tolmachev, *J. Nucl. Med.* **2011**, *52*, 461 – 469.
[34] A. Orlova, T. A. Tran, T. Ekblad, A. E. Karlström, V. Tolmachev, *Eur. J. Nucl. Med. Mol. Imaging* **2010**, *37*, 260 – 269.
[35] M. Altai, H. Wållberg, H. Honarvar, J. Strand, A. Orlova, Z. Varasteh, M. Sandström, J. Löfblom, E. Larsson, S. E. Strand, M. Lubberink, S. Ståhl, V. Tolmachev, *J. Nucl. Med.* **2014**, *55*, 1842 – 1848.
[36] E. Mume, A. Orlova, P. U. Malmström, H. Lundqvist, S. Sjöberg, V. Tolmachev, *Nucl. Med. Biol.* **2005**, *32*, 613 – 622.
[37] J. Feldwisch, V. Tolmachev, *Methods Mol. Biol.* **2012**, *899*, 103 – 126.
[38] S. J. Hosseinimehr, V. Tolmachev, A. Orlova, *Drug Discovery Today* **2012**, *17*, 1224 – 1232.
[39] C. A. Boswell, *J. Med. Chem.* **2013**, *56*, 9418 – 9426 and references therein.

Received: October 28, 2014
Published online on January 12, 2015

